ACS APPLIED MATERIALS & INTERFACES

Research Article

www.acsami.org

Amine Enrichment of Thin-Film Composite Membranes via Low Pressure Plasma Polymerization for Antimicrobial Adhesion

Rackel Reis,*[,†] Ludovic F. Dumée,[‡] Li He,[‡] Fenghua She,[‡] John D. Orbell,[†] Bjorn Winther-Jensen,[§] and Mikel C. Duke[†]

[†]Institute for Sustainability for Innovation, College of Engineering and Science, Victoria University, Hoppers Lane, Werribee, Victoria 3030, Australia

[‡]Institute for Frontier Materials, Deakin University, Pigdons Road, Waurn Ponds,Victoria 3216, Australia

[§]Faculty of Engineering, Monash University, Bayview Avenue, Clayton, Victoria 3800, Australia

Supporting Information

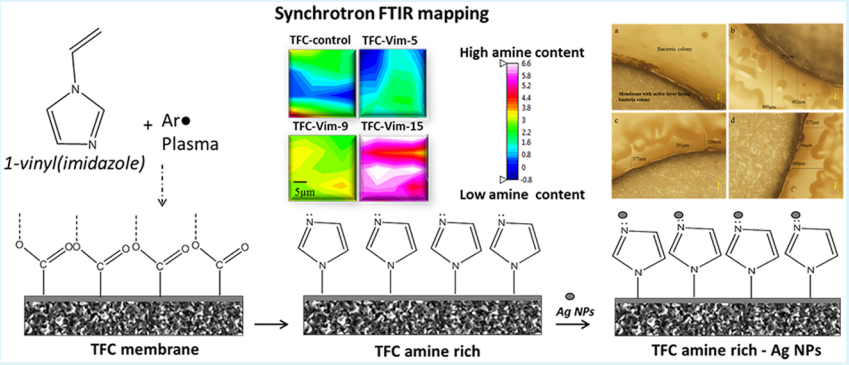

ABSTRACT: Thin-film composite membranes, primarily based on poly(amide) (PA) semipermeable materials, are nowadays the dominant technology used in pressure driven water desalination systems. Despite offering superior water permeation and salt selectivity, their surface properties, such as their charge and roughness, cannot be extensively tuned due to the intrinsic fabrication process of the membranes by interfacial polymerization. The alteration of these properties would lead to a better control of the materials surface zeta potential, which is critical to finely tune selectivity and enhance the membrane materials stability when exposed to complex industrial waste streams. Low pressure plasma was employed to introduce amine functionalities onto the PA surface of commercially available thin-film composite (TFC) membranes. Morphological changes after plasma polymerization were analyzed by SEM and AFM, and average surface roughness decreased by 29%. Amine enrichment provided isoelectric point changes from pH 3.7 to 5.2 for 5 to 15 min of plasma polymerization time. Synchrotron FTIR mappings of the amine-modified surface indicated the addition of a discrete 60 nm film to the PA layer. Furthermore, metal affinity was confirmed by the enhanced binding of silver to the modified surface, supported by an increased antimicrobial functionality with demonstrable elimination of *E. coli* growth. Essential salt rejection was shown minimally compromised for faster polymerization processes. Plasma polymerization is therefore a viable route to producing functional amine enriched thin-film composite PA membrane surfaces.

KEYWORDS: *plasma polymerization, antimicrobial properties, amine enrichment, functional thin-film coatings, nanoscale surface engineering*

INTRODUCTION

TFC membranes are nanostructured materials that are core components in RO desalination technology. These materials are composed of a dense 100−200 nm thick PA film coated onto a mesoporous support layer, typically made of poly(sulfone) (PSf) membrane, supported onto a macroporous poly(ester) backing.[1] The chemistry of the active PA layer governs water and ion transport across the membrane, achieving removal of up to >99% of dissolved salts and organic molecules.[2] In water treatment plants or during industrial wastewater treatment, the PA layer is constantly subjected to a range of stresses associated with water transport under high pressure and exposure to a range of complex contaminants.[3] Over the past four decades, improvements via chemical and fabrication routes have led to RO being the global primary desalination technology. Despite their success, TFC membranes still suffer from issues associated with scaling, fouling (e.g., colloidal, organic, and biofouling), and attack by oxidative

Received: February 19, 2015
Accepted: June 17, 2015
Published: June 17, 2015

DOI: 10.1021/acsami.5b01603
ACS Appl. Mater. Interfaces 2015, 7, 14644−14653

species. The latter may arise from upstream equipment cleaning or water disinfection, affecting flux and rejection performance.[4] Therefore, new routes to further refine their properties are still needed.

Surface modification is one approach to alter surface properties, such as charge and roughness, that can potentially reduce fouling across the surface of membranes.[5,6] Surface morphology and chemical composition play key roles in the physicochemical interactions of the membrane surface with contaminants present in solution.[7] In particular, surface roughness was shown to have a significant impact on fouling mechanisms by facilitating adhesion and cake layer formation on the membrane surface.[8] Evidence of the effect of post-treatment coatings, such as reduced surface roughness, was shown to lead to lower tendencies for organic compound fouling during desalination operation.[9−11] Furthermore, depending on the nature and polarity of such coatings, the surface charge of the modified membranes may be finely altered. In addition, surface charge strongly influences fouling mechanisms and also impacts on single salt permeation and pure water permeability.[12−14] The techniques reported to date for TFC membranes involve chemical grafting polymerization[15,16] and surface coating.[5,17−19] Chemical routes for polymer grafting utilize chemical initiators to generate free-radicals, enabling polymerization of monomers onto the membrane surface.[5,20] This technique was shown to lead to an improved flux during organic fouling tests carried out under operating conditions, due to repulsive interfacial interactions by grafted functionalities.[21] However, the adhesive interactions between polymer and monomer mostly depend on the choice of a suitable monomer to react with chemical groups present on the material.[22] Surface coatings, on the other hand, may lead to covalent immobilization of large macromolecules containing a number of specific functionalities.[5,23] Typically, surface coatings involve several steps whereby the polycondensation of the monomers leads to the formation of a high-density layer. The dense surface coating may cross-polymerize within the top surface of the bulk supporting material, which may largely compromise the materials permeation properties.[17] Therefore, although surface modifications across TFC membranes were shown to improve fouling resistance by altering specific interactions with contaminants, the adverse impact of the coatings on the membrane's performance and chemical stability therefore requires a controlled incorporation of functional groups across the surface of the materials to be treated.[24,25]

Low pressure plasma is a rapidly developing surface modification technique that has been used for almost four decades across a range of different industries.[26−29] In membrane technology, plasma treatment has been intensively studied over the last two decades in attempts to increase the hydrophilicity and improve the low-fouling properties of ultra- and microfiltration membranes.[25] A challenge in applying plasma polymerization to TFC membranes is the difficulty of characterizing the plasma polymerized coatings, since the functionalities of the polymerized surface can be unpredictably rearranged.[30] Furthermore, the substrate has to be subjected to vacuum conditions during the plasma process, which can cause capillary stresses across the pores of the membrane material and ultimately impact liquid permeability.[31−33] Polymerization of monomers is induced by plasma-generated free-radicals formed in a plasma chamber and on the material's surface.[34,35] Low pressure conditions allow the control of the polymerization conditions and thus of the introduced moieties, which leads to typically more stable and uniform thin-films, independently of the deposited monomer and the reactivity of the substrate. A few works have reported on the plasma polymerization of TFC membranes. These studies involved the grafting of hydroxyl-based monomers in order to improve hydrophilicity, a pathway for reducing fouling or scaling by favoring wettability.[36−38] Another group of compounds, such as amines, have previously been demonstrated to act as surface primers to improve the adhesion and stability of hydrophilic coatings (e.g., poly(ethylene) glycol (PEGs) or poly(glycerol)).[21,39] Plasma polymerization of amine functionalities such as allylamine and acrylonitrile has previously been used for TFC fabrication via plasma polymerization, to form active top layers.[40−42] Poly(acrylonitrile) (PAN)-based TFC membranes have been prepared via plasma polymerization, which has been commercialized by Sumitomo Co. as Solrox.[43] Amine coatings, such as *N*-vinylimidazole, offer a promising functionality known for having a strong affinity with metals such as silver, which can potentially introduce antimicrobial properties and possible metal selectivity properties for metal contaminated wastewater separation.[44,45]

In this work, the active PA layer of a commercial TFC membrane was directly functionalized with amine moieties by plasma polymerization of 1-vinylimidazole (VIm) monomers. The resulting amine enrichment presents a versatile platform for further functional modifications including attachment of silver nanoparticles (Ag NPs), conferring measurable antimicrobial activity. The surface and metallic attachment properties of the novel material were comprehensively characterized, and the impact of the modification on the essential membrane performance was also assessed.

MATERIALS AND METHODS

Reagents and materials. BW30 TFC and PSf membranes were purchased from Dow Filmtec Corp. (IMCD limited Australia) and Beijing Puqirui (MWCO 30,000−50,000) technology, respectively. Prior to the plasma treatment BW30 membranes were soaked in DI water for 5 h in order to remove preservative materials and then dried in air. Reagents 1-vinyl imidazole (VIm) for plasma polymerization and Luria−Bertani agar for bacterial assessment were purchased from Sigma-Aldrich. Ag NPs (average 20 nm diameter coated with 0.3 wt % of Poly(vinylpyrrolidone) (PVP)) were purchased from Nano-structured & Amorphous Materials, INC.

Plasma polymerization technique. The monomer VIm was plasma polymerized using a low-power plasma system reported in detail elsewhere.[46] In this work, plasma polymerization was performed initially on a PSf membrane to assess chemical changes before treating the TFC membranes. Membranes were placed separately in the vacuum chamber (2 L) and firmly attached using sticky tape onto a support, exposing the active side only. The plasma polymerization process was divided into three stages inside the chamber, i.e. (i) vacuum conditioning stage: the system was pumped down from an initial Ar gas environment to 5 Pa; (ii) polymerization stage: VIm monomer was injected into the system together with Ar gas to a pressure of 7 Pa. The flow rate was 1.60 mL/min and energy delivered was 1 W/L. At this stage the time exposure could be controlled, being a crucial parameter for generation of free-radicals on the membrane surface and for the control of the etching effect; (iii) reaction stage: the Ar plasma is switched off allowing completion of the reaction involving the monomer.

Silver attachment on TFC membranes. Amine rich and pristine TFC membranes were immersed separately into an Ag NP solution (0.1 mM, 50 mL) for 12 h, rinsed with DI water and dried in 35°. Membranes were then subjected to microbial adherence assessment and silver evaluation with XPS and EDS analysis. Three plasma polymerization times of 5, 9, and 15 min were used on both PSf and

DOI: 10.1021/acsami.5b01603
ACS Appl. Mater. Interfaces 2015, 7, 14644−14653

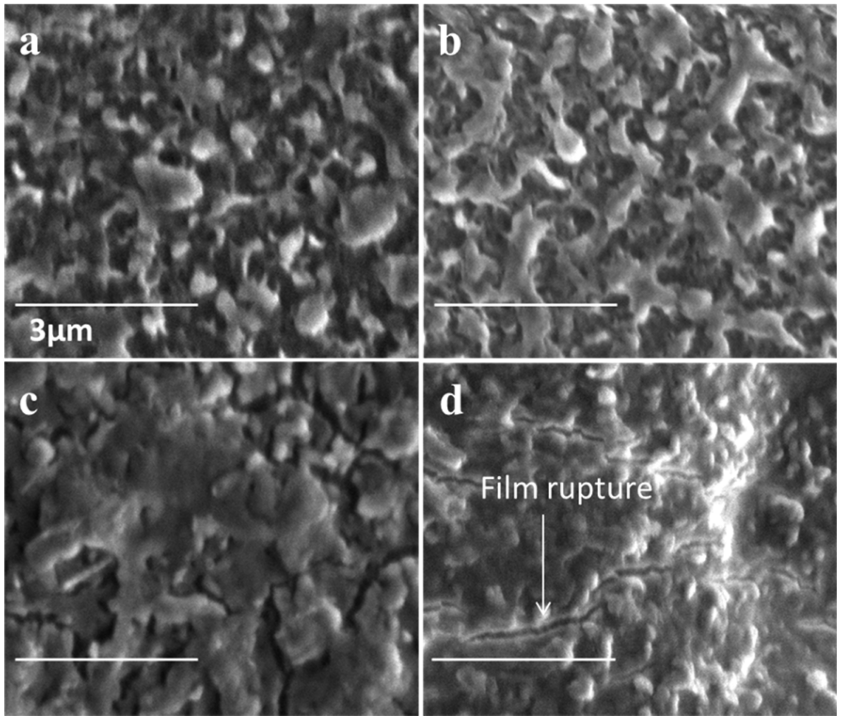

Figure 1. SEM morphology analysis with progressive smoother surface images for TFC membranes: a) TFC-pristine, b) TFC-VIm-5, c) TFC-VIm-9 and d) TFC-VIm-15 with film rupture effect.

TFC membranes. To ensure correct assessment of the plasma effect, a control sample was produced, which was a pristine membrane which was inserted into the plasma vacuum chamber with only the vacuum conditioning stage performed.

Characterization of amine rich TFC membranes. Amine rich surfaces were first characterized with synchrotron Attenuated Total Reflection-Fourier Transform Infrared Spectroscopy ATR-FTIR at the Australian Synchrotron (AS) and then in our laboratory. For the samples analyzed at the AS, single spectra and mapping analysis were performed using a Bruker Hyperion 2000 coupled to laser V80v, MCT narrow band 50 μm detector and spectrometer equipped with an ATR element (45° multireflection germanium and BaF_2 as background). Mapping analysis investigated the distribution of cross-linking functional groups across the surface and estimated amine rich coating thickness. The thickness was evaluated using eq 1 where absorbance intensity from new functionalities observed after plasma was correlated according to the IR depth from the given frequency.

$$\ln\left[\frac{A_t}{A_0}\right] = \frac{2t}{dp} \quad (1)$$

where t = the thickness of the coated film; A = the IR absorbance; and dp = the depth of the IR beam.

All spectra for mapping analysis were collected with a 20 μm knife-edge aperture, corresponding to a 5 × 5 μm spot through the crystal across a wavenumber range of 4000−850 cm^{-1}. For each measurement point, 64 spectra were averaged at resolution of 4 cm^{-1}, background was collected every 5 spectra and analyzed with OPUS 7.2 software from Bruker Corporation.

The surface charge of the amine rich TFC membranes was evaluated with a Surpass Anton Paar Electro Kinetic Analyzer (EKA) utilizing Visiolab software (version 2.2). In the EKA analyzer, membranes were placed onto a 20 mm × 10 mm adjustable gap cell of thickness <2 mm. The streaming channel dimension was approximately 0.1 mm. The pH electrodes (Schott Instruments) were used for measuring of zeta potential at pressure increments from 20 mbar to 500 mbar. A KCl 1 mM solution was used, and 0.1 M HCl and NaOH were used for pH adjustment. An average value of the zeta potential was calculated based on four repeat measurements obtained from both directions of flow in the cell.

Scanning electron micrograph (SEM) images were obtained with a Quanta dual beam Gallium (Ga) Focus Ion Beam (FIB) from FEI and samples were coated with carbon prior to image analysis. The images for SEM mapping were collected under 20 keV with working distance of 10 mm.

Atomic Force Microscopy (AFM) analysis was performed in tapping mode using a Bruker equipped with Nanoscope V multimode scan coupled with a microscope camera 10xA Nikon series 110422. The resonance frequency and force constant for the probe was 300 kHz (±100 kHz) and 40 N/m. Data were collected using Nanoscope 8.4 software, a scan size of 7 μm and images were evaluated using Gwyddion.36 data analysis software.

X-ray photoelectron spectroscopy (XPS) was performed using XPS Spectrometer Kratos AXIS Nova (Kratos Analytical Ltd, Manchester, UK) with aluminium Kα radiation as the X-ray source (1486 eV) at La Trobe University, Victoria Australia University, Victoria Australia. XPS Spectrometer with aluminum K_α radiation as the X-ray source (1486 eV). A quantitative elemental composition of the modified PA was provided for a surface depth of 1−5 nm. The technique was able to detect PA elements and silver concentration with detection limits of 0.1% of the bulk material.

Membrane performance test. Salt rejection and water permeation performance were tested with a laboratory-scale cross-flow filtration system (CF042, Sterlitech Corp., WA, USA). The concentrated feed stream containing sodium chloride (2000 ppm at 25 °C) was pumped to the system with an effective membrane area of 42 cm^2 and flowing tangentially across the membrane surface under 15 bar and trans-membrane pressures were monitored and maintained at the target working pressure within a ± 2% accuracy. The outlet permeate flow was collected after 180 min and salt rejection conductivity measured immediately after the test. Salt concentration was determined using an electrical conductivity meter (Hach HQ40d) and mass of permeate was measured with a balance (EJ-410) and a webcam was used to record at specific interval of 1 min the corresponding mass.

Salt rejection R (%) was calculated according to

DOI: 10.1021/acsami.5b01603
ACS Appl. Mater. Interfaces 2015, 7, 14644−14653

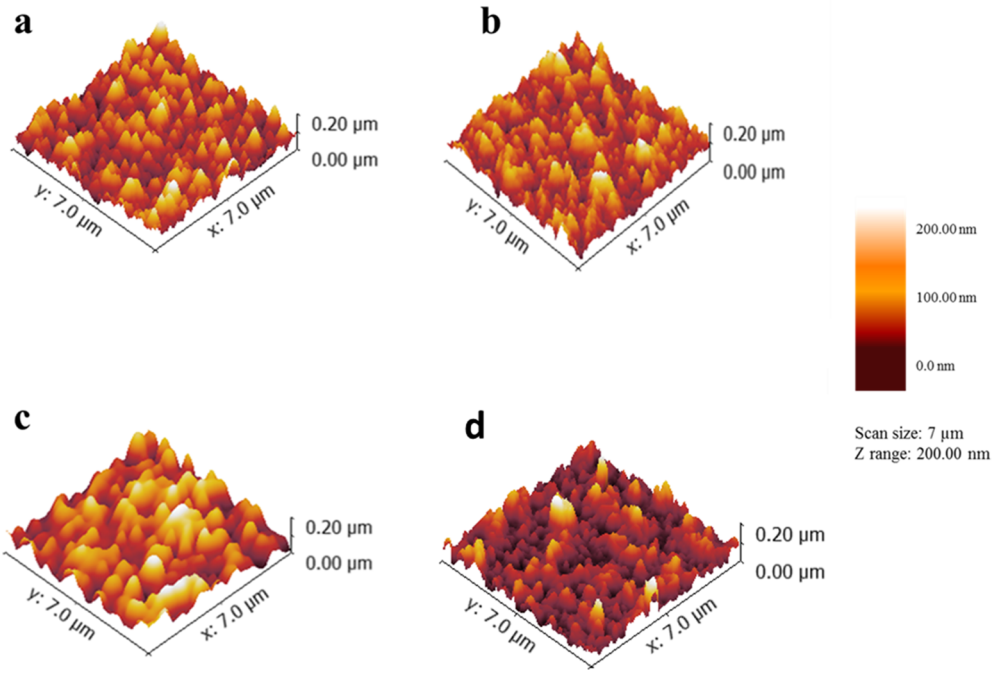

Figure 2. AFM morphology analysis and roughness values: (a) TFC-pristine (rms 31 ± 0.4; R_a 24 ± 0.2), (b) TFC-Vim-5 (rms 27 ± 0.7; R_a 22 ± 0.3), (c) TFC-Vim-9 (rms 29 ± 0.1; R_a 23 ± 0.5), and (d) TFC-Vim-15 (rms 24 ± 0.6; R_a 17 ± 0.4).

$$R = 1 - \left(\frac{C_{permeate}}{C_{feed}}\right) \times 100\% \quad (2)$$

where $C_{permeate}$ and C_{feed} are the conductivity of salt concentration in the permeate and feed, respectively, in μS/cm. Permeate flux F (L/m^2·h^{-1}) was calculated by

$$F = \frac{V}{A \times t} \quad (3)$$

where V is permeate volume (L), A is effective membrane area (m^2), and t is the time over which the volume V was collected (h).

Bacterial adherence assessment. The antimicrobial property on the membrane surface was assessed by exposing the active side of the membrane to *Escherichia coli* (*E. coli* strain Nissle 1917). First, *E. coli* was prepared following the same protocol as previously reported.[47] Functionalized membranes were exposed to *E. coli*, and a 100 μL aliquot of the *E. coli* suspension was pipetted onto an agar plate and then spread over the surface. The membranes (7 mm diameter disk) were placed onto the bacteria-agar surface with the silver-embedded side facing the agar and incubated for 24 h at 37 °C. An optical microscope, coupled with an Olympus DP70 Digital Microscope Camera, was used to image the Petri dishes and quantify antimicrobial inhibition zones around functionalized membranes (at 20 and 50 times magnification). The inhibition zone distances were averaged from five perpendicular points and measured according to the image size of 300 pixels/cm.

RESULTS AND DISCUSSION

Characterization of physical surface properties after plasma polymerization of TFC membranes. Topographical analysis by SEM was performed on amine rich TFC membranes in and membranes exposed to argon plasma alone in order to visually observe the surface characteristics caused by the polymerization. SEM images in Figure 1 show a consistent trend for a smoothing effect after polymerization with increased plasma exposure time. Smoother surfaces became more evident between 9 and 15 min membrane exposure times in contrast to membranes exposed to only argon (Figure S1), where no significant smoothing effect was found. Figure 1d shows superficial amine film rupture for 15 min membrane exposure, suggesting, i.e., (i) mechanical rupture caused by volume change when moved between ambient pressure and vacuum from plasma or SEM; (ii) chemical etching from reactions with the carrier gas causing ablation on a PA surface; or (iii) internal stress in the PA structure due to longer polymerization and thicker coating film. The first possibility may not significantly contribute to the rupture effect once all membranes, including pristine, were exposed to vacuum conditions for both plasma and SEM. The second possibility relates to chemical etching, commonly attributed in sputtering process or *sputter coating*. In sputtering processes, electrons have high mobility; however, ionic species in cold plasma have a low kinetic energy which allows polymerization with preservation of functional groups, without causing surface ablation.[46,48−50] In the third possibility, the internal stress effect is more conclusive, where significant rupture was only found with the thicker film for 15 min of polymerization. This effect was previously observed during studies of the transport characteristic of radicals during plasma polymerization, and the final deposited film thickness was shown to be largely correlated to the deposition duration.[50]

The smoothing effect was also observed from AFM, as shown in Figure 2. A decrease in surface roughness occurred with longer plasma polymerization times. The average roughness (R_a) and roughness mean square (R_{ms}) were calculated from three different locations on the membrane surface. For the pristine TFC membrane, R_a was 24 ± 0.2 nm and R_{ms} was 31 ± 0.4 nm. A slight decrease was found for TFC-VIm-5 (R_a 22 ± 0.3 nm; R_{ms} 27 ± 0.7 nm) and TFC-VIm-9 (R_a 23 ± 0.5 nm; R_{ms} 29 ± 0.1 nm). For TFC-VIm-15 (R_a 17 ± 0.4 nm; R_{ms} 24 ± 0.1 nm) the smoothing effect was more significant, suggesting a potential thicker polymerized layer on the surface. The effect of increasing thickness will be explored in the FTIR analysis.

Given that plasma polymerization allows deposition of thin-films without penetrating the bulk material, the internal stress

DOI: 10.1021/acsami.5b01603
ACS Appl. Mater. Interfaces 2015, 7, 14644−14653

effect as found in SEM analysis (Figure 1d) may suggest that the PA layer was also ruptured with a resultant exposed PSf underlayer. This effect was mostly evident for the 15 min polymerization. However, ruptures may have also occurred for the shorter time plasma polymerized samples.

Quantitative elemental analysis performed with XPS in order to evaluate chemical bonds rupture is shown in Table 1. The XPS elemental analysis can detect up to 5 nm in depth the 200 nm PA layer. Previous XPS performed on the pristine BW30 membrane was shown to lead to the detection of only carbon (C), nitrogen (N), oxygen (O), and very low (S) contents from the PSf supporting layer underneath.[51] The spectra obtained for the plasma polymerized samples showed 10% increase in the N/C elemental ratio expected from the polymerization of the VIm monomer. However, uniquely for plasma polymerized membranes, the S/C ratio also increased by 2 to 9% (Table 2 and Table S1). Increased S content suggests that the PSf underlayer became more apparent to XPS due to small ruptures during plasma polymerization which may adversely affect the selectivity of the TFC membranes. In this respect, the duration of the plasma polymerization process controlled the film thickness, as posteriorly discussed in the IR mapping analysis and shown in Table 1. The duration of the polymerization contributed to increasing film thickness and potential decrease of the stability of the deposited film. Therefore, the alterations in the selectivity can relate to the morphology of the ruptures (depth) and the density of the ruptures, with a certain amount that may interfere with the selectivity.

Table 1. Correlation of Membrane Flux with Chemical/ Physical Properties after Plasma Polymerization

membranes	TFC-VIm[a] N/C ratio (at %)	TFC-VIm film thickness (nm)	TFC-VIm avg roughness R_a (nm)
TFC-dried	0.03	0	24
TFC-VIm-5	0.2	<21	22
TFC-VIm-9	0.2	21	23
TFC-VIm-15	0.2	60	17

[a]Results for XPS analysis were only performed in plasma polymerization of VIm on TFC membranes.

Table 2. Correlation of Selectivity with Chemical Properties after Plasma Polymerization

membranes	TFC-VIm[a] S/C ratio (at %)	TFC-VIm salt rejection (%)	TFC-Argon salt rejection (%)
TFC-control	0.01	97.8 ± 0.5	97.8 ± 0.5
TFC-VIm-5	0.03	95.5 ± 0.7	97.9 ± 0.1
TFC-VIm-9	0.06	95.8 ± 0.4	98.8 ± 0.3
TFC-VIm-15	0.08	93.8 ± 0.4	98.1 ± 0.1

[a]Results for XPS analysis were only performed in plasma polymerization of VIm on TFC membranes.

The performance test is an essential parameter to verify the feasibility of the plasma technique on TFC membranes. In order to detect the impact of plasma conditions, including the plasma etching effect, on the modified membrane's performance, plasma polymerized membranes were compared to a series of control membranes, as shown in Figure 3a: i.e. (i) pristine membrane tested under "as supplied" conditions; (ii) dried pristine that had only been dried in air for 12 h; (iii) pristine membrane that had been subjected to vacuum conditions from the plasma chamber; and (iv) membranes exposed to argon plasma, used as the carrier gas in the plasma polymerization process.

In terms of salt rejection, the fixed argon plasma conditions did not affect the membrane's selectivity, given that rejections were maintained in the range of 98 to 99% for all plasma durations (Figure 3a). However, in the plasma polymerization process, selectivity declined similarly for the time range between 5 and 9 min (95.5% and 95.7%). For 15 min of treatment, the rejection was found to decline to 93.8%, approximately 4% lower than that of the pristine membrane: 97.8% ± 0.5. The drop in salt rejection suggests an association of factors that influenced the PA selectivity, such as film rupture (as mentioned in SEM analysis) and surface charge, as demonstrated in the next section.

The film rupture potentially introduced larger pores on the PA layer, allowing larger salt molecules to diffuse across the exposed nonselective PSf layer—confirmed with increased S/C ratio as correlated in Table 2. For the 5 and 9 min membranes, the thin amine film delivered nanosized ruptures near the PA

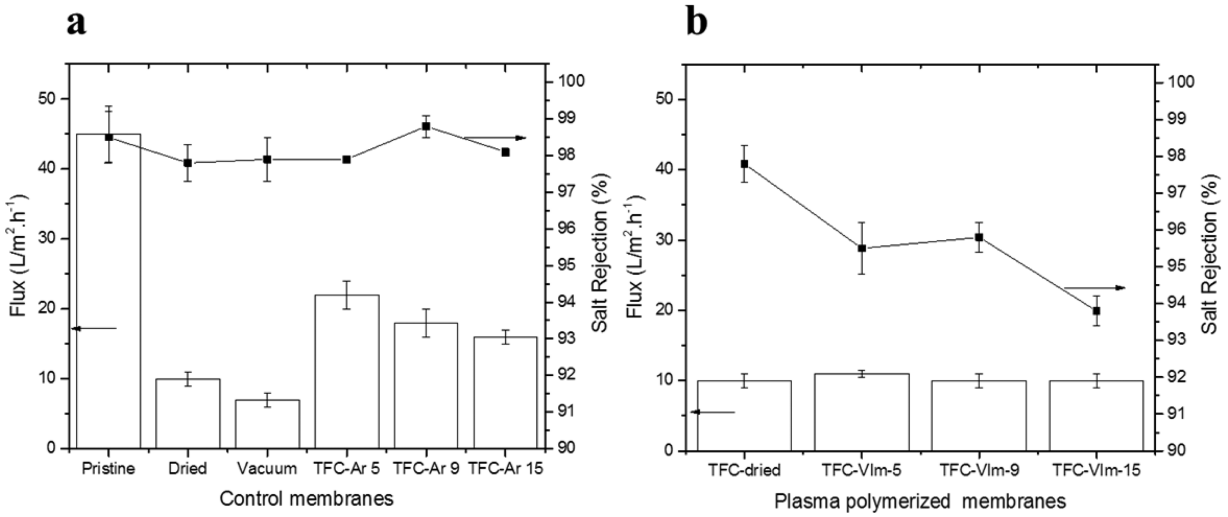

Figure 3. Permeation test for controls and modified membranes under 15 bar inlet pressure and 2000 ppm of NaCl solution: 27 °C at pH 6.5. (a) series of control membranes and argon plasma; (b) amine rich modified membranes.

DOI: 10.1021/acsami.5b01603
ACS Appl. Mater. Interfaces 2015, 7, 14644−14653

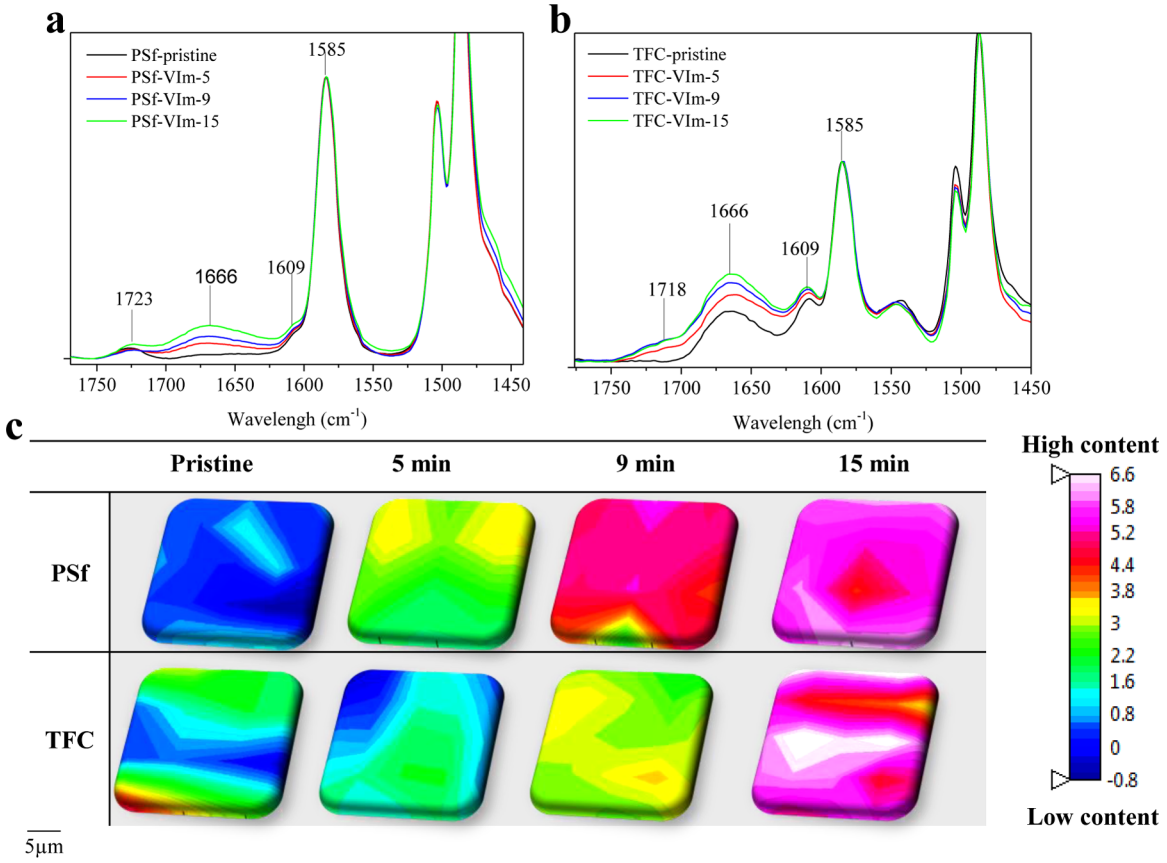

Figure 4. ATR-FTIR peak profile for absorption bands noted after plasma polymerization: (a) peaks at 1724 to 1666 cm^{-1} for PSf and (b) at 1716 cm^{-1} to 1666 cm^{-1} for TFC. (c) SIR-Map homogeneity analysis with integration of peak 1666 cm^{-1}.

layer and lowered both salt rejections by 2%. For 15 min, the film deposition appeared to have more penetrating ruptures but only enough to lower salt rejection by 4%. The selectivity drops from the 5 and 9 min membranes were still very close to the variations of the RO membrane under a variety of system conditions and configurations.[52]

The pristine membranes under air- and vacuum-dried conditions showed flux decline by 78%. The membranes exposed to argon plasma did not show superior decline than the dried pristine with flux drops around 60 to 64% (Figure 3a), which led to the conclusion that flux was not altered by plasma. Furthermore, the flux of the plasma polymerized membranes presented in Figure 3b showed a similar average flux decline trend to that of dried control membranes. Therefore, the impact on the flux was more associated with the degree of dryness of the material than with the low pressure plasma polymerization process.[32] The drying step prior to the plasma process suggests an effect of membrane voids collapse that led to flux loss.[31] Therefore, cleaning procedures, including solvent exchange and atmospheric pressure conditions for plasma polymerization of TFC membranes, may lead to less impact on membrane permeation once no drying step is required.[37,33,53]

Characterization of amine moiety distribution and chemical properties after plasma polymerization. The amine thin-film chemical profile was investigated with ATR-FTIR analysis of modified PSf as a reference material (Figure 4a), TFC membrane (Figure 4b), and TFC membrane exposed to only argon plasma (Figure S2). Cross-linking bonds were identified with the formation of a broad band corresponding to a carbonyl (C═O) stretching vibration around 1723 cm^{-1}, an amide I (C−N) stretching vibration at 1666 cm^{-1}, and an aromatic amide (N−H) deformation vibration or C═C ring stretching vibration 1609 cm^{-1}.[54,55] The carbonyl band was formed after plasma polymerization from the reaction of free-radicals generated by the plasma via atmospheric O_2, a common reaction found in any polymer after plasma polymerization.[50] In the amide I band, possible cross-linking related to rearranged and ruptured imidazole rings present within the monomer was detected on the surface. As an example, amide I stretching vibrations were previously reported at the frequencies of 1663 and 1668 cm^{-1}. The band 1666 cm^{-1} was reported for pyrimidine, an aromatic heterocyclic organic compound similar to the imidazole ring present within the monomer.[56] The same bands corresponding to cross-linked bonds were also found for amine rich TFC membranes, as shown in Figure 4b. However, no significant alterations were found for membranes exposed to argon plasma alone, which confirms that the enhanced bands are correlated to polymerization on the surface. The duration of the plasma polymerization was varied for both the PSf and TFC membranes in an attempt to alter the amine coverage. The area of peak 1666 cm^{-1} was plotted in contour color maps to evaluate the homogeneity of the chemical distributions on the surface of the materials. Thus, synchrotron ATR-FTIR mapping, Figure 4c, shows the amine group content for both of these membranes after different treatment times, with respect to the absorption at 1666 cm^{-1}. This peak was found to proportionally increase with longer plasma treatment times for both PSf and TFC membrane materials. Equation 1 was used to estimate the thickness of the plasma coating by evaluating the penetration depth of the infrared beam across this particular

DOI: 10.1021/acsami.5b01603
ACS Appl. Mater. Interfaces 2015, 7, 14644−14653

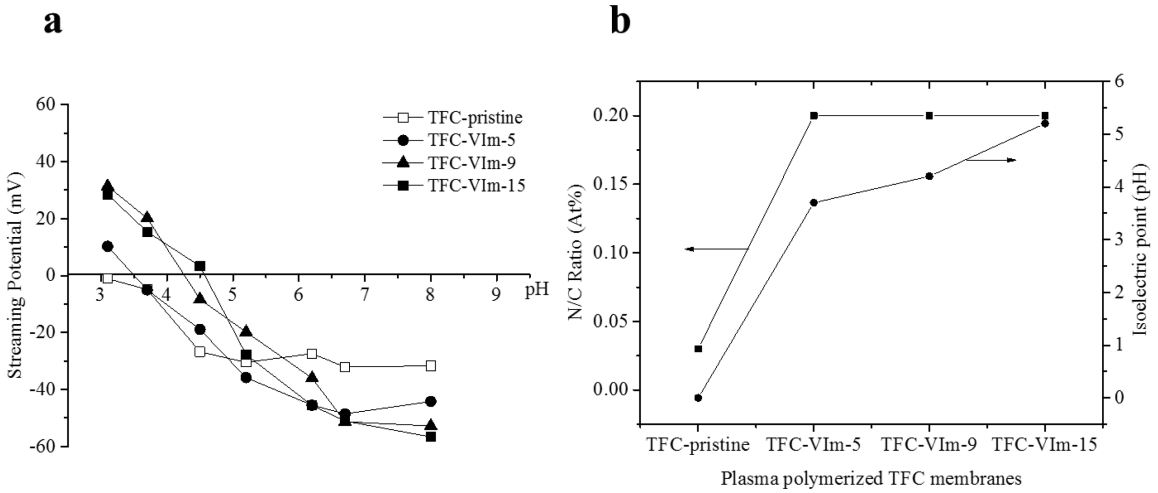

Figure 5. (a) Streaming potential for TFC-pristine with isoelectric point for amine rich membranes between pH 3.7 and 5.2. (b) Correlation between increased amine groups detected by streaming potential and increased N/C ratio detected by XPS after plasma polymerization.

wavelength range.[57] The degree of amine enrichment for the PSf membrane was estimated to be between 250 nm, 290 nm, and 345 nm for 5, 9, and 15 min plasma polymerization times, respectively.

Higher amine densities could be measured for the TFC membranes as a result of plasma polymerization, particularly between 9 and 15 min. This corresponded to thicknesses of 21 and 60 nm, respectively. The 5 min of plasma polymerization duration offered the least amine enrichment coverage, and the thickness of the layer could not be satisfactory evaluated. The density of the C−N stretching vibration as seen on the contour plot map before plasma polymerization showed irregular distribution across the surface of pristine TFC membranes. However, after plasma polymerization, the density of these functionalities increased with longer plasma polymerization times, leading to a more homogeneous distribution—this was especially evident after 15 min.

The surface charge was also investigated as a function of pH (Figure 5) in order to set the best conditions for selectivity of modified membranes. This analysis highlights the protonation and deprotonation of amine groups and nascent carboxylic groups on the surface. Polymeric membrane materials are charged when in contact with an aqueous medium.[58] Electrostatic interactions between the solution and the membrane result in an electric double layer, and the resultant charge on the surface can be evaluated as the zeta potential. The zeta potential is dependent on the compositions of the membrane surface and the ambient solution. For this reason, this analysis was also performed for pristine and TFC membranes exposed to argon plasma alone (Figure S3) in order to investigate chemical reactions promoted by the polymerization process. The curve profile for a pristine membrane shows a flat negatively charged surface (∼30 mV) over the pH range of 3 to 9.[59] For amine rich surfaces, at low pH, the magnitude of positive charge increased with increasing plasma time compared to the control, most notably between 5 and 9 min (15 min yielded a similar surface property to 9 min). This can be attributed to the protonation of the added functional amine groups due to plasma polymerization. Furthermore, the isoelectric points were found at pH 3.7 for 5 min, and for 9 and 15 min exposures, they increased to 4.7 and 5.2, respectively, consistent with an increase of basic amine mieties on the surface. On the other hand, as pH increased from 6, all amine rich samples showed proportional surface charges increasing in magnitude of negative charge between −40 and −50 mV at pH 8. This effect is more reflective of the deprotonation of amine groups and nascent carboxylates groups.[60] Another potential contribution is associated with formed carboxylates upon reaction with air after removal from the plasma chamber, which is supported by the increased carboxylic bands shown in Figure 4b. The membranes exposed to argon plasma alone showed a similar curve profile to that of the pristine, with slightly increased magnitude of negative charge (∼ −40 mV at pH 8), while the influence of negative charge was more attributed to available nascent carboxylic groups. The increased amine presence on the surface is also consistent with the increase in the N/C ratio, as measured by XPS (Figure 5b). Furthermore, selectivity was affected for the denser amine coverage of the 9 and 15 min membranes in different intensities. As the feed solution was ∼6, the 15 min membrane operated under the influence of the IEP at pH 5.2. Minimum rejections can occur with feed solution either at or above one or two pH units higher than the IEP.[61,62] Therefore, results led to agreement that 9 min is the optimum time with potential pH operation conditions in the alkaline range.

Characterization of attached silver nanoparticles on the amine rich TFC membranes. The membranes confirmed to have increased amine functionalities were then exposed to silver nanoparticles to explore the novel metal binding mechanism. The enhanced binding of silver was shown in a wide scan XPS spectrum, Figure S4b, as compared to the pristine membrane (Figure S4a). As a further confirmation of the silver presence, a closer analysis of the silver peak (Figure S4c) shows the Ag_{3d} core level spectrum split into two peaks at 372 and 366 eV, indicating Ag $3d_{5/2}$ and Ag $3d_{3/2}$, respectively.[63] The percentage of silver was 6% by wt (or 1 at % equivalent) (Table S1) measured by EDS (Figure S5) at 3 keV.

The silver functionalized membranes were tested for antimicrobial properties by exposure to *E. coli*. A number of studies have correlated the silver ions release with the bacteria elimination mechanism and, as well, the biocidal lifespan.[45] The release rates are mainly influenced by the particle size and pH conditions, although some limitations on the methodology for separation of nanoparticles and ions prior to detection potentially can led to experimental artifacts.[64] The particle

DOI: 10.1021/acsami.5b01603
ACS Appl. Mater. Interfaces 2015, 7, 14644−14653

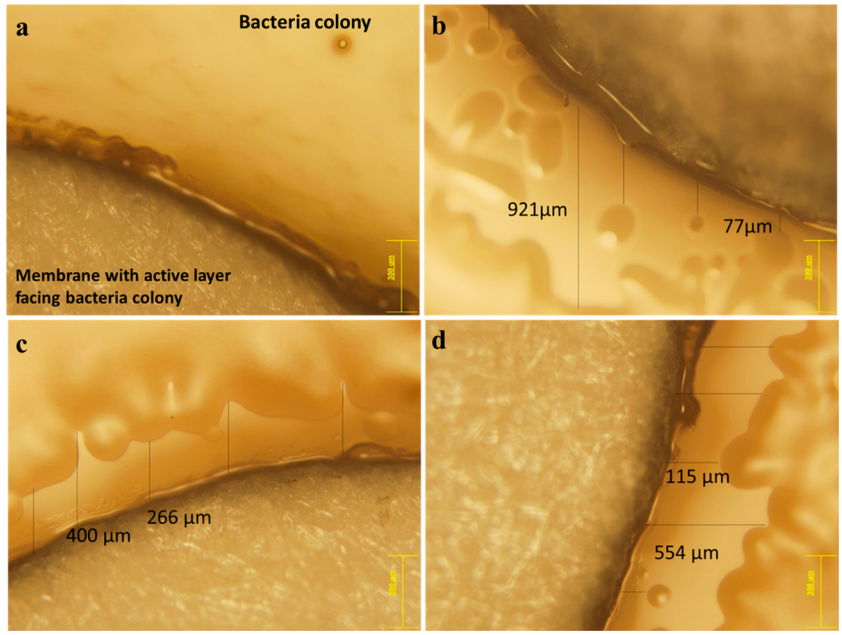

Figure 6. Bacteria assessment with increased inhibition zone distance associated with amine rich and Ag NPs attached on membrane surfaces: (a) TFC-pristine, (b) TFC-VIm-5Ag, (c) TFC-VIm-9Ag, and (d) TFC-VIm-15Ag.

etching is time dependent over a 6−24 h observation period.[65] For particles around 20 nm under neutral aqueous medium as used in this study, fast biocidal activity (~2−4 nm/h) enabled elimination of bacteria in the first 5 h and elimination maintained within 24 h.[66,67] Inhibition zones indicating antimicrobial activity are shown in Figure 6. The inhibition zone showed different distance ranges which could be potentially caused by the aggregation/agglomeration of the Ag NPs, and therefore, the average was measured from five points. The pristine membrane, Figure 6a, shows a dense bacterial area with no inhibition zone. For the 5 min plasma exposure membrane treated with silver, inhibition zones started to appear, in contrast to the bacteria-free valleys that are clearly identified as dispersed "bubbles", and the average was 304 μm with minimum distance of 77 μm. For 9 and 15 min (Figure 6c and 6d), inhibition zones were more defined with an average of 342 and 330 μm and minimum distances of 266 and 115 μm, respectively. The amine enrichment was therefore found to be directly correlated to the diameter of the inhibition zones and also showed minimum distances were less likely for longer polymerization times. This suggests that longer plasma polymerization durations lead to more coordination sites being available for silver attachment.

While the silver attachment and associated antimicrobial functionality have been demonstrated, the effect of leaching over time is an important issue. Silver leaching from chemically modified silver nanoparticles bonded to the surface of TFC membranes showed Ag^+ release lasting months during operational cross-flow filtration.[68] This indicates that silver modified membranes may require reloading of silver nanoparticles, possibly during routine cleaning of the operating membrane plant. Therefore, further research is needed to investigate the long-term stability of the attached amine groups, as well as the attached silver nanoparticles, during operation conditions to confirm the viability of plasma polymerization for improved performance of TFC membranes.

CONCLUSIONS

Plasma polymerization demonstrated feasibility for adherence of amine functionality onto PA layer in thin-film composite membrane. The coating thickness was readily controlled by exposure time, which influences film density and homogeneity. An increasing value for the surface isoelectric point with increasing polymerization time was consistent with increasing amine enrichment which it benchmarked optimum pH conditions suitable for amine rich membranes. Enhanced metal binding to the added amine groups was demonstrated with silver nanoparticles, where antimicrobial property was confirmed.

ASSOCIATED CONTENT

Supporting Information

Figure S1: SEM topographical analysis of TFC membranes exposed to argon plasma Figure S2: ATR-FTIR analysis of TFC membranes exposed to argon plasma Figure S3: Streaming potential analysis for membranes exposed to argon plasma Figure S4: XPS analysis of silver peak and Ag 3d core level Figure S5: EDS spectra of silver peak Table S1: XPS contents from plasma polymerized membranes and Ag NPs attachment "This material is available free of charge via the Internet at http://pubs.acs.org/."The Supporting Information is available free of charge on the ACS Publications website at DOI: 10.1021/acsami.5b01603.

AUTHOR INFORMATION

Corresponding Author

*E-mail: rackel.reis@live.vu.edu.au; Tel: +61406903950.

Notes

The authors declare no competing financial interest.

ACKNOWLEDGMENTS

The authors would like to acknowledge Ph.D. stipend and project funding from the Collaborative Research Network initiative of the Australian Department of Industry. R.R.

DOI: 10.1021/acsami.5b01603
ACS Appl. Mater. Interfaces 2015, 7, 14644−14653

acknowledges the postgraduate top up scholarship from the National Centre of Excellence in Desalination Australia, funded by the Australian Government through the National Urban Water and Desalination Plan. The authors also acknowledge Mark Tobin, Lilijana Puskar, and Danielle Martin from the Australian Synchrotron (Melbourne), Robert Jones from Centre for Materials and Surface Science, Department of Physics in La Trobe University, Bao Lin for AFM contribution, Maëlle Lemoing from Deakin University for bacteria assessment, and Jianhua Zhang from Victoria University for access to the filtration system.

REFERENCES

(1) Cadotte, J. E.; Petersen, R. J.; Larson, R. E.; Erickson, E. E. A New Thin-film Composite Seawater Reverse Osmosis Membrane. *Desalination* **1980**, *32*, 25−31.

(2) Lee, K. P.; Arnot, T. C.; Mattia, D. A Review of Reverse Osmosis Membrane Materials for Desalination Development to Date and Future Potential. *J. Membr. Sci.* **2011**, *370*, 1−22.

(3) Kagramanov, G. G.; Farnosova, E. N. Effect of Solution Composition on Selectivity of Reverse Osmosis and Nanofiltration Membranes. *Pet. Chem.* **2012**, *52*, 625−630.

(4) Do, V. T.; Tang, C. Y.; Reinhard, M.; Leckie, J. O. Effects of Chlorine Exposure Conditions on Physiochemical Properties and Performance of a Polyamide Membrane-Mechanisms and Implications. *Environ. Sci. Technol.* **2012**, *46*, 13184−13192.

(5) Bhattacharya, A.; Rawlins, J. W.; Ray, P. *Polymer grafting and crosslinking*; Wiley Online Library: 2009.

(6) Kang, G.-D.; Cao, Y.-M. Development of antifouling reverseosmosis membranes for water treatment: a review. *Water Res.* **2012**, *46*, 584−600.

(7) Gao, Y.; Haavisto, S.; Li, W.; Tang, C. Y.; Salmela, J.; Fane, A. G. Novel Approach To Characterizing the Growth of a Fouling Layer during Membrane Filtration via Optical Coherence Tomography. *Environ. Sci. Technol.* **2014**, *48*, 14273−14281.

(8) Vrijenhoek, E. M.; Elimelech, M.; Hong, S. Influence of membrane surface properties on initial rate of colloidal fouling of reverse osmosis and nanofiltration membranes. *J. Membr. Sci.* **2001**, *188*, 115−128.

(9) Baek, Y.; Yu, J.; Kim, S.-H.; Lee, S.; Yoon, J. Effect of Surface Properties of Reverse Osmosis Membranes on Biofouling Occurrence under Filtration Conditions. *J. Membr. Sci.* **2011**, *382*, 91−99.

(10) Rana, D.; Matsuura, T. Surface Modifications for Antifouling Membranes. *Chem. Rev. (Washington, DC, U. S.)* **2010**, *110*, 2448−2471.

(11) Subramani, A.; Huang, X.; Hoek, E. M. V. Direct Observation of Bacterial Deposition onto Clean and Organic-fouled Polyamide Membranes. *J. Colloid Interface Sci.* **2009**, *336*, 13−20.

(12) Childress, A. E.; Elimelech, M. Relating Nanofiltration Membrane Performance to Membrane Charge (Electrokinetic) Characteristics. *Environ. Sci. Technol.* **2000**, *34*, 3710−3716.

(13) Coronell, O.; Mariñas, B. J.; Cahill, D. G. Accessibility and Ion Exchange Stoichiometry of Ionized Carboxylic Groups in the Active Layer of FT30 Reverse Osmosis Membrane. *Environ. Sci. Technol.* **2009**, *43*, 5042−5048.

(14) Lee, W.; Ahn, C. H.; Hong, S.; Kim, S.; Lee, S.; Baek, Y.; Yoon, J. Evaluation of Surface Properties of Reverse Osmosis Membranes on the Initial Biofouling Stages under no Filtration Condition. *J. Membr. Sci.* **2010**, *351*, 112−122.

(15) Blok, A. J.; Chhasatia, R.; Dilag, J.; Ellis, A. V. Surface Initiated Polydopamine Grafted Poly([2-(methacryoyloxy)ethyl]-trimethylammonium chloride) Coatings to Produce Reverse Osmosis Desalination Membranes with Anti-Biofouling Properties. *J. Membr. Sci.* **2014**, *468*, 216−223.

(16) Rana, H. H.; Saha, N. K.; Jewrajka, S. K.; Reddy, A. V. R. Low Fouling and Improved Chlorine Resistant Thin-film Composite Reverse Osmosis Membranes by Cerium(IV)/Polyvinyl Alcohol Mediated Surface Modification. *Desalination* **2015**, *357*, 93−103.

(17) Louie, J. S.; Pinnau, I.; Ciobanu, I.; Ishida, K. P.; Ng, A.; Reinhard, M. Effects of Polyether−polyamide Block Copolymer Coating on Performance and Fouling of Reverse Osmosis Membranes. *J. Membr. Sci.* **2006**, *280*, 762−770.

(18) Sarkar, A.; Carver, P. I.; Zhang, T.; Merrington, A.; Bruza, K. J.; Rousseau, J. L.; Keinath, S. E.; Dvornic, P. R. Dendrimer-based Coatings for Surface Modification of Polyamide Reverse Osmosis Membranes. *J. Membr. Sci.* **2010**, *349*, 421−428.

(19) Yu, S.; Lü, Z.; Chen, Z.; Liu, X.; Liu, M.; Gao, C. Surface modification of thin-film composite polyamide reverse osmosis membranes by coating n-isopropylacrylamide-co-acrylic acid copolymers for improved membrane properties. *J. Membr. Sci.* **2011**, *371*, 293−306.

(20) Gilron, J.; Belfer, S.; Vaisanen, P.; Nystrom, M. Effects of Surface Modification on Antifouling and Performance Properties of Reverse Osmosis Membranes. *Desalination* **2001**, *140*, 167−179.

(21) Jaleh Mansouri, S. H.; Chen, Vicki Strategies for Biofouling in Membrane Filtration Systems: Challenges and Opportinities. *J. Mater. Chem.* **2010**, *20*, 4567−4567.

(22) Louie, J. S.; Pinnau, I.; Reinhard, M. Effects of Surface Coating Process Conditions on the Water Permeation and Salt Rejection Properties of Composite Polyamide Reverse Osmosis Membranes. *J. Membr. Sci.* **2011**, *367*, 249−255.

(23) Karamdoust, S.; Yu, B.; Bonduelle, C. V.; Liu, Y.; Davidson, G.; Stojcevic, G.; Yang, J.; Lau, W. M.; Gillies, E. R. Preparation of Antibacterial Surfaces by Hyperthermal Hydrogen Induced Cross-Linking of Polymer Thin Films. *J. Mater. Chem.* **2012**, *22*, 4881−4889.

(24) Khulbe, K. C.; Feng, C.; Matsuura, T. The Art of Surface Modification of Synthetic Polymeric Membranes. *J. Appl. Polym. Sci.* **2010**, *115*, 855−895.

(25) Kochkodan, V.; Johnson, D. J.; Hilal, N. Polymeric Membranes: Surface Modification for Minimizing (bio)Colloidal Fouling. *Adv. Colloid Interface Sci.* **2014**, *206*, 116−140.

(26) Borcia, C.; Borcia, G.; Dumitrascu, N. Relating plasma surface modification to polymer characteristics. *Appl. Phys. A: Mater. Sci. Process.* **2008**, *90*, 507−515.

(27) Chang, J. P.; Coburn, J. W. Plasma−surface interactions. *J. Vac. Sci. Technol., A* **2003**, *21*, 145−151.

(28) Fridman, A. *Plasma Chemistry*; Cambridge University: New York, 2008. http://VU.eblib.com.au/patron/FullRecord.aspx?p=343495.

(29) Zhang, R.; Guo, X.; Shi, X.; Sun, A.; Wang, L.; Xiao, T.; Tang, Z.; Pan, D.; Li, D.; Chen, J. Highly Permselective Membrane Surface Modification by Cold Plasma-Induced Grafting Polymerization of Molecularly Imprinted Polymer for Recognition of Pyrethroid Insecticides in Fish. *Anal. Chem. (Washington, DC, U. S.)* **2014**, *86*, 11705−11713.

(30) Yasuda, H. K. Some Important Aspects of Plasma Polymerization. *Plasma Processes Polym.* **2005**, *2*, 293−304.

(31) Albo, J.; Wang, J.; Tsuru, T. Application of Interfacially Polymerized Polyamide Composite Membranes to Isopropanol Dehydration: Effect of Membrane Pre-treatment and Temperature. *J. Membr. Sci.* **2014**, *453*, 384−393.

(32) Filmtec, D. *Handling, Preservation and Storage: Re-wetting of Dried Out Elements*; Home Page.http://msdssearch.dow.com/PublishedLiteratureDOWCOM/dh_003c/0901b8038003cdeb.pdf?filepath=liquidseps/pdfs/noreg/609-02105.pdf (accessed Mar, 2014).

(33) Porter, M. C. *Handbook of industrial membrane technology*; Noyes Publications: NJ, 1989; pp 143.

(34) Ershov, S.; Khelifa, F.; Dubois, P.; Snyders, R. Derivatization of Free Radicals in an Isopropanol Plasma Polymer Film: The First Step toward Polymer Grafting. *ACS Appl. Mater. Interfaces* **2013**, *5*, 4216−4223.

(35) Khelifa, F.; Ershov, S.; Habibi, Y.; Snyders, R.; Dubois, P. Use of Free Radicals on the Surface of Plasma Polymer for the Initiation of a Polymerization Reaction. *ACS Appl. Mater. Interfaces* **2013**, *5*, 11569−11577.

DOI: 10.1021/acsami.5b01603
ACS Appl. Mater. Interfaces 2015, 7, 14644−14653

(36) Kim, E.-S.; Yu, Q.; Deng, B. Plasma Surface Modification of Nanofiltration (NF) Thin-Film Composite (TFC) Membranes to Improve Anti Organic Fouling. *Appl. Surf. Sci.* **2011**, *257*, 9863−9871.
(37) Kim, M.-M.; Lin, N. H.; Lewis, G. T.; Cohen, Y. Surface Nano-Structuring of Reverse Osmosis Membranes Via Atmospheric Pressure Plasma-Induced Graft Polymerization for Reduction of Mineral Scaling Propensity. *J. Membr. Sci.* **2010**, *354*, 142−149.
(38) Zou, L.; Vidalis, I.; Steele, D.; Michelmore, A.; Low, S. P.; Verberk, J. Q. J. C. Surface Hydrophilic Modification of RO Membranes by Plasma Polymerization for Low Organic Fouling. *J. Membr. Sci.* **2011**, *369*, 420−428.
(39) Romero-Vargas Castrillón, S.; Lu, X.; Shaffer, D. L.; Elimelech, M. Amine Enrichment and Poly(ethylene glycol) (PEG) Surface Modification of Thin-film Composite Forward Osmosis Membranes for Organic Fouling Control. *J. Membr. Sci.* **2014**, *450*, 331−339.
(40) Hollahan, J. R.; Wydeven, T. Synthesis of Reverse Osmosis Membranes by Plasma Polymerization of Allylamine. *Science* **1973**, *179*, 500−501.
(41) Peric, D.; Bell, A. T.; Shen, M. Reverse Osmosis Characteristics of Composite Membranes Prepared by Plasma Polymerization of Allylamine. Effects of Deposition Conditions. *J. Appl. Polym. Sci.* **1977**, *21*, 2661−2673.
(42) Suzuki, S.; Ogawa, T.,Hitotsuyanagi, N. Plasma-polymerized Membranes of 4-Vinylpyridine in Reverse Osmosis. In *Reverse Osmosis and Ultrafiltration*; American Chemical Society: 1985; Chapter 6, pp 69−82.
(43) Murase, I.; Takao, S.,Tsutsui, N. Process for Producing Polyacrylonitrile Reverse Osmotic Membranes. U.S.4283359 A, 1981.
(44) El-Hamshary, H.; Fouda, M. M. G.; Moydeen, M.; Al-Deyab, S. S. Removal of Heavy Metal Using Poly (N-vinylimidazole)-Grafted-Carboxymethylated Starch. *Int. J. Biol. Macromol.* **2014**, *66*, 289−294.
(45) Welles, A. E. *Silver Nanoparticles: Properties, Characterization and Applications*; Nova Science Publishers, Inc.: Hauppauge, NY, USA, 2010.
(46) Norrman, K.; Winther-Jensen, B. Controlling the Plasma-polymerization Process of N-Vinyl-2-pyrrolidone. *Plasma Processes Polym.* **2005**, *2*, 414−423.
(47) Dumee, L. F.; He, L.; King, P. C.; Moing, M. L.; Guller, I.; Duke, M.; Hodgson, P. D.; Gray, S.; Poole, A. J.; Kong, L. Towards Integrated Anti-microbial Capabilities: Novel Bio-Fouling Resistant Membranes by High Velocity Embedment of Silver Particles. *J. Membr. Sci.* **2015**, *475*, 552−561.
(48) Vandencasteele, N.; Reniers, F. Plasma-modified polymer surfaces: characterization using XPS. *J. Electron Spectrosc. Relat. Phenom.* **2010**, *178−179*, 394−408.
(49) Winther-Jensen, B.; Norrman, K.; Kingshott, P.; West, K. Characterization of Plasma-polymerized Fused Polycyclic Compounds for Binding Conducting Polymers. *Plasma Processes Polym.* **2005**, *2*, 319−327.
(50) Yasuda, H. *Plasma polymerization*; Academic Press, Inc.: Orlando, FL 32887, 1985.
(51) Tang, C. Y.; Kwon, Y.-N.; Leckie, J. O. Probing the nano and micro-scales of reverse osmosis membranes - a comprehensive characterization of physiochemical properties of uncoated and coated membranes by XPS, TEM, ATR-FTIR, and streaming potential measurements. *J. Membr. Sci.* **2007**, *287*, 146−156.
(52) Filmtec, D. Desalination Technologies and Filtration Processes; Home Page on the Web. http://msdssearch.dow.com/PublishedLiteratureDOWCOM/dh_0042/0901b80380042dd2.pdf?filepath=liquidseps/pdfs/noreg/609-02002.pdf (accessed Jan, 2013).
(53) Tendero, C.; Tixier, C.; Tristant, P.; Desmaison, J.; Leprince, P. Atmospheric Pressure Plasmas: A Review. *Spectrochim. Acta, Part B* **2006**, *61*, 2−30.
(54) Tang, C. Y.; Kwon, Y.-N.; Leckie, J. O. Effect of membrane chemistry and coating layer on physiochemical properties of thin film composite polyamide RO and NF membranes: I. FTIR and XPS characterization of polyamide and coating layer chemistry. *Desalination* **2009**, *242*, 149−167.
(55) Wu, S.; Zheng, G.; Lian, H.; Xing, J.; Shen, L. Chlorination and Oxidation of Aromatic Polyamides. I. Synthesis and Characterization of Some Aromatic Polyamides. *J. Appl. Polym. Sci.* **1996**, *61*, 415−420.
(56) Haris, P. I.; Severcan, F.; Press, I. O. S. *Vibrational Spectroscopy in Diagnosis and Screening*; IOS Press: Amsterdam, 2012.
(57) Singh, P. S.; Joshi, S. V.; Trivedi, J. J.; Devmurari, C. V.; Rao, A. P.; Ghosh, P. K. Probing the Structural Variations of Thin-film Composite RO Membranes Obtained by Coating Polyamide over Polysulfone Membranes of Different Pore Dimensions. *J. Membr. Sci.* **2006**, *278*, 19−25.
(58) Tang, C. Y.; Kwon, Y.-N.; Leckie, J. O. The Role of Foulant−foulant Electrostatic Interaction on Limiting Flux for RO and NF Membranes During Humic Acid Fouling—Theoretical Basis, Experimental Evidence, and AFM Interaction Force Measurement. *J. Membr. Sci.* **2009**, *326*, 526−532.
(59) Tang, C. Y.; Kwon, Y.-N.; Leckie, J. O. Effect of Membranes Chemistry and Coating Layer on Physiochemical Properties of Thin-film Composite Polyamide RO and NF membranes: II Membrane Physiochemical Properties and their Dependence on Polyamide and Coating Layers. *Desalination* **2009**, *242*, 168−182.
(60) Romero-Vargas Castrillón, S.; Lu, X.; Shaffer, D. L.; Elimelech, M. Amine Enrichment and Poly(ethylene glycol) (PEG) Surface Modification of Thin-film Composite Forward Osmosis Membranes for Organic Fouling Control. *J. Membr. Sci.* **2014**, *450*, 331−339.
(61) Mullett, M.; Fornarelli, R.; Ralph, D. Nanofiltration of Mine Water: Impact of Feed pH and Membrane Charge on Resource Recovery and Water Discharge. *Membranes* **2014**, *4*, 163−180.
(62) Zhong, C.-M.; Xu, Z.-L.; Fang, X.-H.; Cheng, L. Treatment of Acid Mine Drainage (AMD) by Ultra-low-pressure Reverse Osmosis and Nanofiltration. *Environ. Eng. Sci.* **2007**, *24*, 1297−1306.
(63) Fu, Y.; Li, G.; Tian, M.; Wang, X.; Zhang, L.; Wang, W. Preparation of Silver Nanoparticle Immobilized Fibrillar Silicate by Poly(dopamine) Surface Functionalization. *J. Appl. Polym. Sci.* **2014**, DOI: 10.1002/app.39859.
(64) Rizzello, L.; Pompa, P. P. Nanosilver-based Antibacterial Drugs and Devices: Mechanisms, Methodological Drawbacks, and Guidelines. *Chem. Soc. Rev.* **2014**, *43*, 1501−1518.
(65) Wang, X.; Ji, Z.; Chang, C. H.; Zhang, H.; Wang, M.; Liao, Y.-P.; Lin, S.; Meng, H.; Li, R.; Sun, B.; Winkle, L. V.; Pinkerton, K. E.; Zink, J. I.; Xia, T.; Nel, A. E. Use of Coated Silver Nanoparticles to Understand the Relationship of Particle Dissolution and Bioavailability to Cell and Lung Toxicological Potential. *Small* **2014**, *10*, 385−398.
(66) Liu, J.; Sonshine, D. A.; Shervani, S.; Hurt, R. H. Controlled Release of Biologically Active Silver from Nanosilver Surfaces. *ACS Nano* **2010**, *4*, 6903−6913.
(67) Mitrano, D.; Ranville, J. F.; Stephan, C.,Shelton, C. *Quantitative Evaluation of Nanoparticle Dissolution Kinetics Using Single Particle ICP-MS: A Case Study with Silver Nanoparticles*; http://www.perkinelmer.com/CMSResources/Images/44-158789APP_NexION-350Q-Silver-Nanoparticles-Dissolution-Kinetics_011750_01.pdf.
(68) Yin, J.; Yang, Y.; Hu, Z.; Deng, B. Attachment of silver nanoparticles (AgNPs) onto thin-film composite (TFC) membranes through covalent bonding to reduce membrane biofouling. *J. Membr. Sci.* **2013**, *441*, 73−82.

DOI: 10.1021/acsami.5b01603
ACS Appl. Mater. Interfaces 2015, 7, 14644−14653